

采用薄层氮化碳促进的高性能钯基催化剂用于甲酸分解制氢

孙志聪^{1,2,3}, 罗二桂^{1,2,3}, 孟庆磊^{1,2,3}, 王显^{1,2,3}, 葛君杰^{1,2,3,*}, 刘长鹏^{1,2,3,*}, 邢巍^{1,2,4,*}

¹中国科学院长春应用化学研究所先进电源实验室, 长春 130022

²中国科学技术大学, 应用化学与工程学院, 合肥 230026

³吉林省低碳化学电源重点实验室, 长春 130022

⁴中国科学院长春应用化学研究所电分析化学国家重点实验室, 长春 130022

High-Performance Palladium-Based Catalyst Boosted by Thin-layered Carbon Nitride for Hydrogen Generation from Formic Acid

Zhicong Sun^{1,2,3}, Ergui Luo^{1,2,3}, Qinglei Meng^{1,2,3}, Xian Wang^{1,2,3}, Junjie Ge^{1,2,3,*},
Changpeng Liu^{1,2,3,*}, Wei Xing^{1,2,4,*}

¹ Laboratory of Advanced Power Sources, Changchun Institute of Applied Chemistry, Chinese Academy of Sciences, Changchun 130022, P. R. China.

² University of Science and Technology of China, College of Applied Chemistry and Engineering, Hefei 230026, P. R. China.

³ Jilin Province Key Laboratory of Low Carbon Chemical Power Sources, Changchun 130022, P. R. China.

⁴ State Key Laboratory of Electroanalytical Chemistry, Changchun Institute of Applied Chemistry, Chinese Academy of Sciences, Changchun 130022, P. R. China.

*Corresponding authors. Emails: liuchp@ciac.ac.cn (C.L.); xingwei@ciac.ac.cn (W.X.); gejj@ciac.ac.cn (J.G.).

Tel.: +86-431-85262225 (C.L.); +86-431-85262223 (W.X.); +86-431-85262225 (J.G.).

1 Chemicals and materials

Trithiocyanuric acid (AR) was provided by JK scientific Co., Ltd. Melamine (AR), formic acid (AR) purchased from Aladdin Co. Sodium hydroxide (AR) and HCl were purchased from Beijing Chemical Works. Sodium formate dehydrate (AR) were purchased from sinopharm Chemical Reagent Co., Ltd. Vulcan carbon powder XC-72 was provided by Cabot Co. Highly purified argon ($\geq 99.99\%$) was supplied by Changchun Juyang Co Ltd. Ultrapure water (resistivity: $\rho \geq 18 \text{ M}\Omega\cdot\text{cm}^{-1}$) was used to prepare the solutions. PdCl_2 was dissolved into $0.1 \text{ mol}\cdot\text{L}^{-1}$ HCl aqueous solution to obtain H_2PdCl_4 solution.

2 Material characterization

An XL 30 ESEM-FEG field emission scanning electron microscope was used to measure Scanning electron microscopy (SEM) images. Transmission electron microscopy (TEM), high-angle annular dark-field scanning transmission electron microscopy (HAADF-STEM) and element mapping analysis were performed on Philips TECNAI G2 electron microscope at 200 kV. Power X-ray diffraction (XRD) measurements were performed on D8 ADVANCE diffractometer (BRUKER Co.) with a $\text{Cu } K\alpha$ ($\lambda = 0.154 \text{ nm}$) radiation source operating at 40 kV. The textural and morphological features of the various carbon supports and catalysts prepared were determined by nitrogen physisorption at 77 K in a Micromeritics ASAP 2020. The composition of the products was determined by an inductively coupled plasma optical emission spectrometer (ICP-OES; X Series 2, Thermo Fisher Scientific, USA). X-ray photoelectron spectroscopy (XPS) measurements were carried out on $\text{Mg } K\alpha$ radiation source (Kratos XSAM-800 spectrometer). The binding energy was calibrated against the C 1s line.

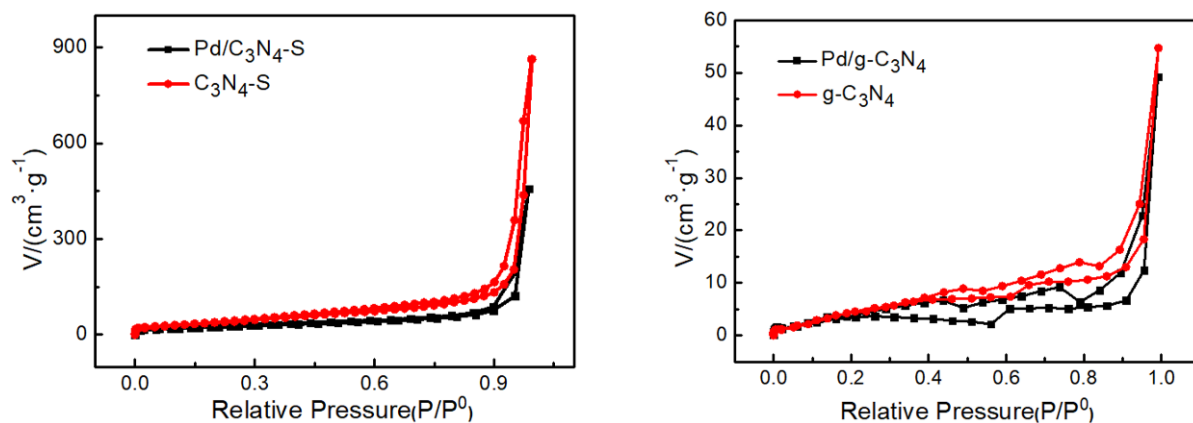


Fig. S1 Nitrogen adsorption-desorption isotherms of C_3N_4 , $\text{C}_3\text{N}_4\text{-S}$, $\text{Pd/C}_3\text{N}_4$ and $\text{Pd/C}_3\text{N}_4\text{-S}$ fitted by the BET (Brunauer-Emmett-Teller) method.

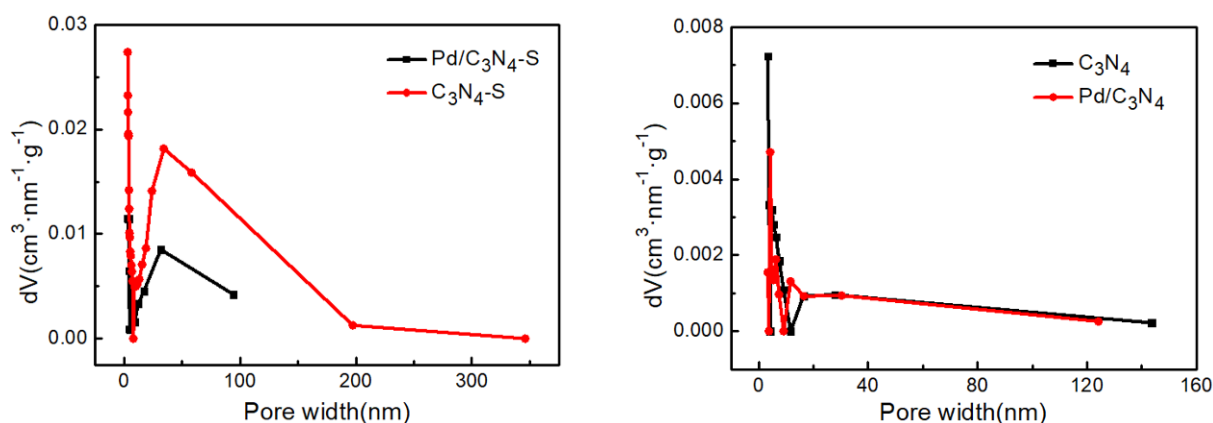


Fig. S2 The pore size distribution of C_3N_4 , $\text{C}_3\text{N}_4\text{-S}$, $\text{Pd/C}_3\text{N}_4$ and $\text{Pd/C}_3\text{N}_4\text{-S}$.

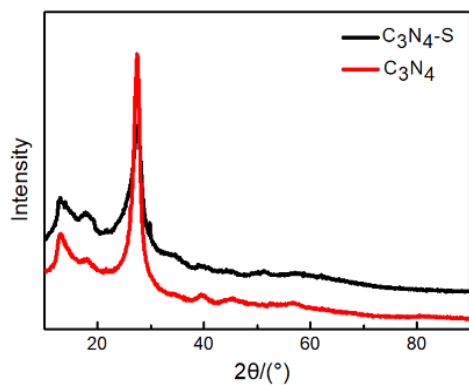


Fig. S3 The XRD full spectra of Pd/C₃N₄ and Pd/C₃N₄-S.

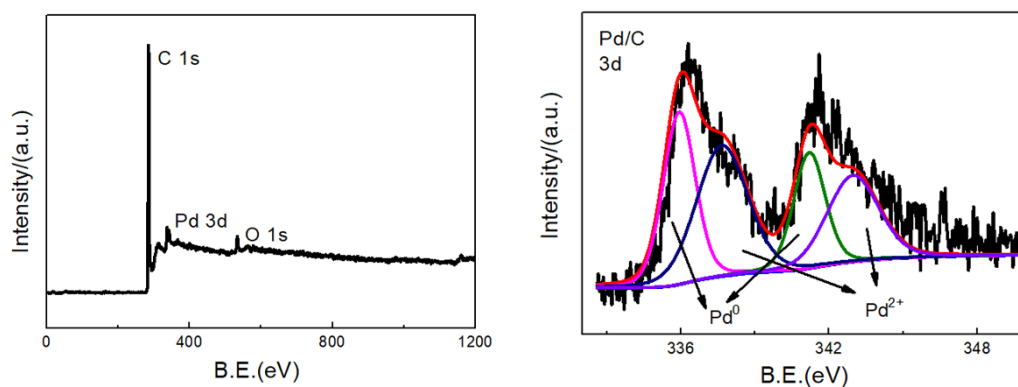


Fig. S4 The XPS spectra of the Pd/C and the Pd 3d XPS spectra of the Pd/C.

Table S1 The content of S element in the support before and after calcination (Determined by elemental analysis test).

Sample	Mass fraction(S)/%	
	before calcination	after calcination
C ₃ N ₄ -S	52.45	0.85

Table S2 The content of each element (2-catalyst indicates that it is prepared by the ethylene glycol microwave reduction method).

Catalyst	Elemental analysis test		ICP-OES test
	Mass fraction(N)/%(support)		Mass fraction(Pd)/%
Pd/C	-		4.12
Pd/C ₃ N ₄	62.17		1.61
2-Pd/C ₃ N ₄	62.17		0.12
Pd/C ₃ N ₄ -S	61.76		3.21
2-Pd/C ₃ N ₄ -S	61.76		0.20

Table S3 The Pd and N atomic contentment on the surface of the samples according to the XPS spectra.

catalyst	Atomic contentment/%				
	Pd ⁰	Pd ²⁺	pyridinic N	pyrrolic N	graphitic N
Pd/C	59.79	40.21	-	-	-
Pd/C ₃ N ₄	45.17	54.83	39.91	41.50	18.59
Pd/C ₃ N ₄ -S	51.89	48.11	40.87	42.76	16.37

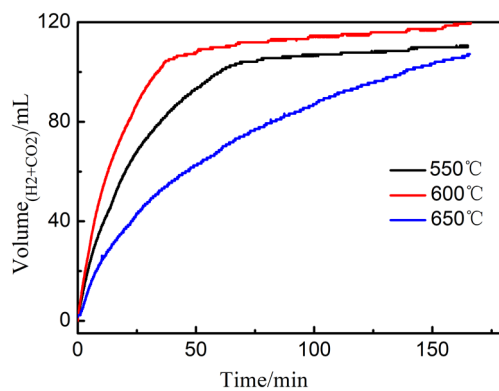


Fig. S5 Pd/C₃N₄-S prepared by using trimeric thiocyanate as precursor at different pyrolysis temperatures and sodium borohydride reduction method.

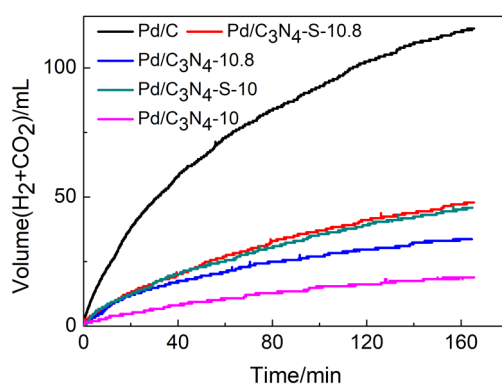


Fig. S6 Formic acid decomposition performance of catalyst prepared by ethylene glycol microwave reduction.

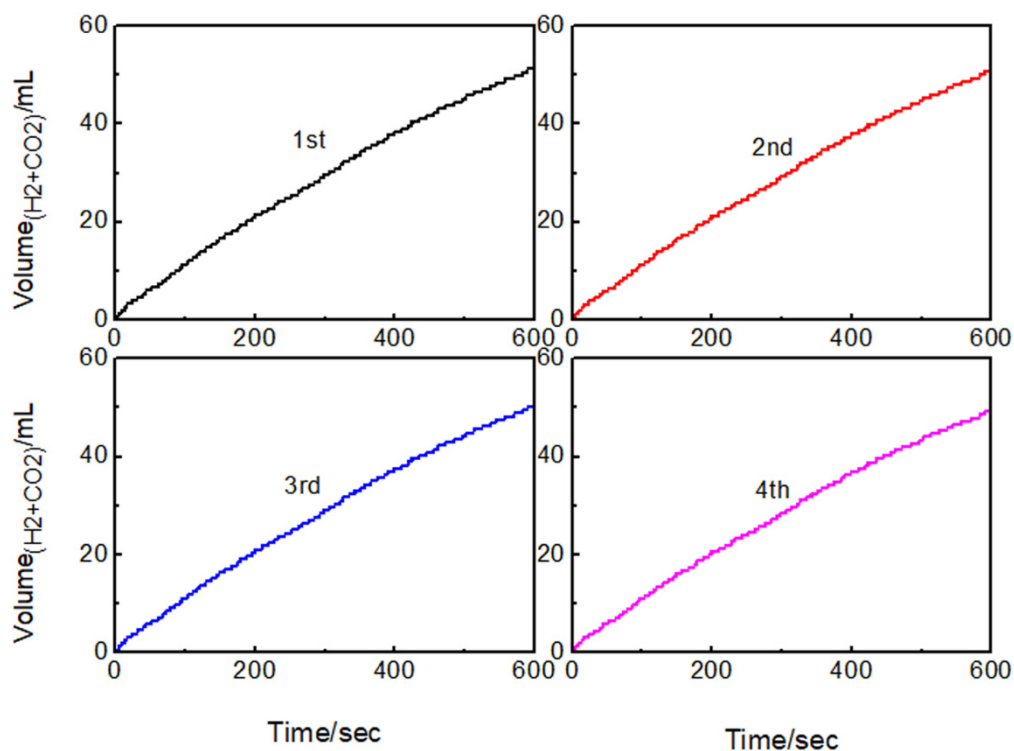


Fig. S7 Cyclic stability of Pd/C₃N₄-S catalyzed formic acid decomposition.

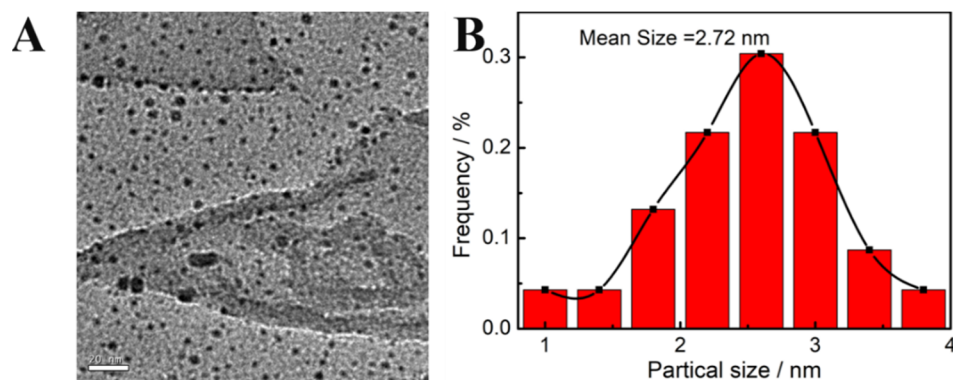


Fig. S8 (A) TEM image of Pd / C₃N₄-S after cyclic stability test; (B) Particle size distribution of Pd NPs of Pd / C₃N₄-S after cyclic stability test.

Table S4 Comparison of the performance of this work with the reported formic acid decomposition catalyst.

Catalyst	Additive	TOF (h ⁻¹)	Mass activity (mol _{H₂} ·g ⁻¹ ·Pd·h ⁻¹)	T/K	Reference
Pd/C ₃ N ₄ -S	SF	2083	19.52	303	This work
PdAu/C-CeO ₂	-	-	2.13	365	S1
Pd/N-MSC-30	SF	8414	7.47	333	S2
Pd/MSC-30	SF	750	3.59	298	S3
Pd-B/C	SF	1184	3.50	303	S4
Pd/r-GO	SF	5420	6.39	353	S5
Pd/CN _{0.25}	-	5530	6.52	298	S6
Pd @ CN	FA	71	0.67	288	S7
Pd/C ₂ F ₈	SF	1166	11.01	303	S8
Pd-M(OH) ₂ /S-1	-	5803	11.91	333	S9
PdO/C	SF	3172	8.72	303	S10
PdAg@ZrO ₂ /C/rGO	SF	4500	-	333	S11
Ag _{0.1} Pd _{0.9} /rGO	SF	2739	2.31	323	S12
Co _{0.30} Au _{0.35} Pd _{0.35} /C	FA	80	0.05	298	S13
Ag ₁ Pd ₉ @NPC	SF	1029		303	S14

Table S5 The content of each component in the gas product determined by gas chromatography (The limit of detection for CO is 0.1 × 10⁻⁶).

Catalyst	Additive	H ₂ /%	CO ₂ /%	O ₂ /%	N ₂ /%	H ₂ : CO ₂	N ₂ : O ₂
Pd/C	SF	46.38	44.60	1.81	7.21	1.04 : 1	3.98 : 1
Pd/C ₃ N ₄ -S	SF	47.51	47.04	1.10	4.44	1.01 : 1	3.94 : 1

Reference

- (S1) Zhou, X.; Huang, Y.; Xing, W.; Liu, C.; Liao, J.; Lu, T. *Chem. Commun.* **2008**, *30*, 3540. doi: 10.1039/B803661F
- (S2) Li, Z.; Yang, X.; Tsumori, N.; Liu, Z.; Himeda, Y.; Autrey, T. *ACS Catal.* **2017**, *7*, 2720. doi: 10.1021/acscatal.7b00053
- (S3) Zhu, Q. -L.; Tsumori, N.; Xu, Q. *Chem. Sci.* **2014**, *5*, 195. doi: 10.1039/C3SC52448E
- (S4) Jiang, K.; Xu, K.; Zou, S.; Cai, W. -B. *J. Am. Chem. Soc.* **2014**, *136*, 4861. doi: 10.1021/ja5008917
- (S5) Bi, Q. -Y.; Lin, J. -D.; Liu, Y. -M.; Du, X. -L.; Wang, J. -Q.; He, H. -Y. *Angew. Chem. Int. Edit.* **2014**, *53*, 13583. doi: 10.1002/anie.201409500
- (S6) Bi, Q. -Y.; Lin, J. -D.; Liu, Y. -M.; He, H. -Y.; Huang, F. -Q.; Cao, Y. *Angew. Chem. Int. Edit.* **2016**, *55*, 11849. doi: 10.1002/anie.201605961
- (S7) Cai, Y. -Y.; Li, X. -H.; Zhang, Y. -N.; Wei, X.; Wang, K. -X.; Chen, J. -S. *Angew. Chem. Int. Edit.* **2013**, *52*, 11822. doi: 10.1002/anie.201304652
- (S8) Wang, X.; Meng, Q.; Liu, C.; Xing, W. *Int. J. Hydrog. Energy* **2019**, *44*, 28402. doi: 10.1016/j.ijhydene.2019.05.083
- (S9) Sun, Q.; Wang, N.; Bing, Q.; Si, R.; Liu, J.; Bai, R. *Chem.* **2017**, *3*, 477. doi: 10.1016/j.chempr.2017.07.001
- (S10) Lv, Q.; Meng, Q.; Liu, W. *J. Phys. Chem. C.* **2018**, *122*, 2081. doi: 10.1021/acs.jpcc.7b08105
- (S11) Song, F. -Z.; Zhu, Q. -L.; Yang, X.; Zhan, W. -W.; Pachfule, P.; Tsumori, N. *Adv. Energy Mater.* **2018**, *8*, 1701416. doi: 10.1002/aenm.201701416
- (S12) Chen, Y.; Zhu, Q. -L.; Tsumori, N.; Xu, Q. *J. Am. Chem. Soc.* **2015**, *137*, 106. doi: 10.1021/ja511511q
- (S13) Wang, Z. -L.; Yan, J. -M.; Ping, Y.; Wang, H. -L.; Zheng, W. -T.; Jiang, Q. *Angew. Chem. Int. Edit.* **2013**, *52*, 4406. doi: 10.1002/anie.201301009
- (S14) Zhang, X.; Shang, N.; Shang, H. *Energy Technol.* **2019**, *7*, 140. doi: 10.1002/ente.201800522